THE JOURNAL OF PHYSICAL CHEMISTRY B

Article

pubs.acs.org/JPCB

Charging Free Energy Calculations Using the Generalized Solvent Boundary Potential (GSBP) and Periodic Boundary Condition: A Comparative Analysis Using Ion Solvation and Oxidation Free Energy in Proteins

Xiya Lu and Qiang Cui*

Department of Chemistry and Theoretical Chemistry Institute, University of Wisconsin—Madison, 1101 University Avenue, Madison, Wisconsin 53706, United States

Supporting Information

ABSTRACT: Free energy simulations using a finite sphere boundary condition rather than a periodic boundary condition (PBC) are attractive in the study of very large biomolecular systems. To understand the quantitative impact of various approximations in such simulations, we compare charging free energies in both solution and protein systems calculated in a linear response framework with the Generalized Solvent Boundary Potential (GSBP) and PBC simulations. For simple ions in solution, we find good agreements between GSBP and PBC charging free energies, once the relevant correction terms are taken into consideration. For PBC simulations with the particle-mesh-Ewald for long-range electrostatics, the contribution (ΔG_{P-M}) due to the use of a particle rather than molecule based summation scheme in real space is found to be significant, as pointed out by Hünenberger and co-workers. For GSBP, when the inner region is close to be charge neutral, the key correction is the overpolarization of water molecules at the inner/outer dielectric boundary; the magnitude of the correction (ΔG_{s-pol}), however, is relatively small. For charging (oxidation) free energy in proteins, the situation is more complex, although good agreement between GSBP and PBC can still be obtained when care is exercised. The smooth dielectric boundary approximation inherent to GSBP tends to make significant errors when the inner region is featured with a high net charge. However, the error can be corrected with Poisson−Boltzmann calculations using snapshots from GSBP simulations in a straightforward and robust manner. Because of the more complex charge and solvent distributions, the magnitudes of ΔG_{P-M} and ΔG_{s-pol} in protein simulations appear to be different from those derived for solution simulations, leading to uncertainty in directly comparing absolute charging free energies from PBC and GSBP simulations for protein systems. The relative charging/oxidation free energies, however, are robust. With the linear response approximation, for the specific protein system (CueR) studied, the effect of freezing the protein structure in the outer region is found to be small, unless a very small (8 Å) inner region is used; even in the latter case, the result is substantially improved when the nearby metal binding loop is allowed to respond to metal oxidation. The implications of these results to the applicability of GSBP to complex biomolecules and in ab initio QM/MM simulations are discussed.

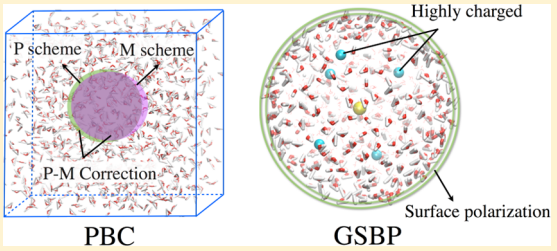

INTRODUCTION

Electrostatic interactions are crucial to the structure and function of biomolecules.[1−3] Numerous efficient computational approaches have been proposed and implemented for calculating electrostatics in complex biomolecular systems. The most widely adopted approach is Ewald summation[4] and its various variations, such as the particle mesh Ewald (PME),[5] in the context of periodic boundary condition (PBC). Potential artifacts associated with the enforced periodicity have been thoroughly discussed in the literature and considered well understood.[6−9] As the system size increases, PBC simulations tend to be computationally demanding; thus, an attractive alternative is to adopt the finite sphere boundary condition, where one describes the key ("inner") region of the system microscopically while the rest (the "outer" region), which generally contains bulk solvent, ions, and the remaining biomolecule, is described with either continuum (macroscopic) electrostatics or a semimacroscopic[10−12] model. A notable example is the Generalized Solvent Boundary Potential (GSBP) approach developed by Roux and co-workers[13] for classical simulations and later adopted by our group[14,15] and others[16] for hybrid QM/MM simulations. By expanding the Green's function for the inner region electrostatic problem with a basis set, the GSBP provides an efficient approach for propagating molecular dynamics trajectories for the region of interest. This makes it possible to compute meaningful free energy changes associated with local events such as binding[17]

Received: October 6, 2012
Revised: January 23, 2013
Published: January 24, 2013

dx.doi.org/10.1021/jp309877z | J. Phys. Chem. B 2013, 117, 2005−2018

and catalysis[18−20] in very large biomolecular systems, such as the ribosome.

Although several studies have carefully analyzed the performance of GSBP based classical[17,21] and QM/MM simulations[16,22,23] for realistic biomolecules, and the general findings support the use of GSBP for processes that localize to regions far (>15−20 Å) from the microscopic/continuum boundary, a direct and systematic comparison between GSBP and PME based free energy simulations has not been carried out. As GSBP gets applied to increasingly complex biomolecules, it is important to understand the impact of various approximations inherent in the model and means to improve the results in quantitative applications. Specifically, the GSBP partitions a solvated macromolecule into the "inner" microscopic region and the "outer" macroscopic (continuum electrostatics) region. The outer region is fixed and described with distinct effective dielectric constants (e.g., 1−4 for the protein and 80 for bulk water), and the interface between the inner and outer regions is also assumed to be fixed and molecularly smooth; this makes it possible to use a basis set expansion for the relevant Green's function. Clearly, GSBP is designed to tackle problems that do not involve large collective motions in the system. Nevertheless, it is important to understand for an apparently local process, such as the oxidation of a metal ion in the active site, what are the consequences of those inherent approximations.

For example, it is well appreciated that macroscopic concepts such as the dielectric "constant" do not readily apply to highly heterogeneous systems like proteins at the molecular scale.[10−12,24−26] Therefore, in principle it is desirable to adopt a more sophisticated dielectric model than a single effective (or empirical) dielectric constant to describe the fixed outer region, whose dielectric response is not explicitly sampled during the simulation. Prior to such development, however, it is important to establish the impact of the outer region; in realistic biomolecules, it is possible that active site properties are largely dictated by nearby interactions and the outer region contribution is effectively screened out by the inner region protein and solvent molecules. Moreover, the approximation of a rigid and smooth dielectric boundary between the inner and outer regions is expected to be most reliable when the net charge of the inner region is conserved; when the net charge changes, such as during oxidation/reduction, (de)protonation or an alchemical mutation that involves charged groups, it is possible that the approximations introduce a significant error that needs to be corrected. It is important to understand when such errors become large and how can they be corrected.

In the current work, we compare GSBP and PBC based protocols for charging free energy simulations in both solution and proteins, although the observations and insights should apply to the general comparison of free energy simulations using finite-sphere versus periodic boundary setups. There are several motivations to focus on charging free energy simulations for this comparative analysis. First, as stated above, the main goal is to understand the impact of various approximations in GSBP; studying processes that involve a net change in the total charge is most revealing in this context. Second, as discussed in great depth in recent studies,[27−36] PME based free energy calculations are subject to several subtleties (although, as also discussed below, the magnitude of correction might be large) when the net charge of the system changes (see Figure 1). Therefore, systematically comparing GSBP and PME results for charging free energy simulations of more diverse systems helps better understand these subtle but important

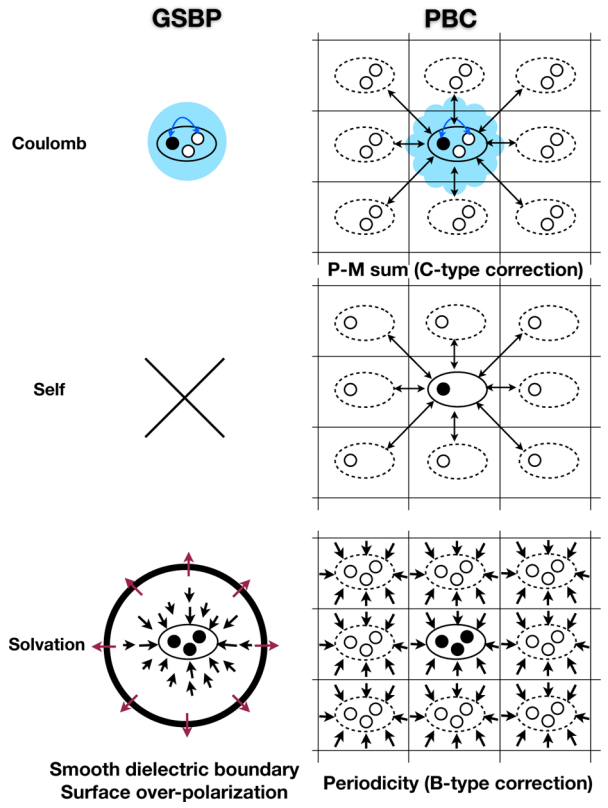

Figure 1. A scheme that illustrates the corrections necessary for GSBP and PBC (PME) simulations for electrostatic free energy simulations (adapted with permission from Figure 1 of ref 8. Copyright 1999 American Institute of Physics). The filled dot indicates the reference charge and unfilled dots for other charges; the single-headed arrows indicate polarization of the nearby solvent/protein dipoles. For PBC (PME) simulations, the corrections need to be considered include[36,49] type B, which is due to the self-energy and periodicity induced solvation terms, and type C, which is due to the use of an inappropriate particle (P) based summation scheme for Coulomb interactions; for systems studied here, only the type C correction (ΔG_{P-M} in Table 2) is found to be large and considered. For GSBP simulations, the corrections include those due to preferentially oriented water molecules (indicated by red arrows) at the inner/outer boundary (i.e., overpolarization, ΔG_{s-pol} in Table 2) and the smooth dielectric boundary approximation (corrected with Poisson−Boltzmann calculations, see Tables 4 and 6).

correction terms. Third, in many realistic applications, the net charge of the system changes; examples include calculations of solvation free energy of ions,[37,38] redox potential[12,39−41] and pK_a[11,22,42] values in solution and proteins, and relative binding energies of ligands that differ in their net charge.[43,44] Finally, from a practical perspective, charging free energy simulations have been shown to often follow linear response,[19,45−47] although care must be taken to establish the validity of the linear response approximation (LRA[48]) for the specific problem in hand[42,46] (see Supporting Information). We adopt the LRA for the current study since it substantially reduces the computational cost for the fairly large protein system we use as the model; we use the LRA for both GSBP and PBC simulations for a consistent comparison.

In the following, we first describe the Computational Methods and simulation details followed by the Results and Discussions section. We summarize this work with conclusions in the Concluding Remarks section.

dx.doi.org/10.1021/jp309877z | J. Phys. Chem. B 2013, 117, 2005−2018

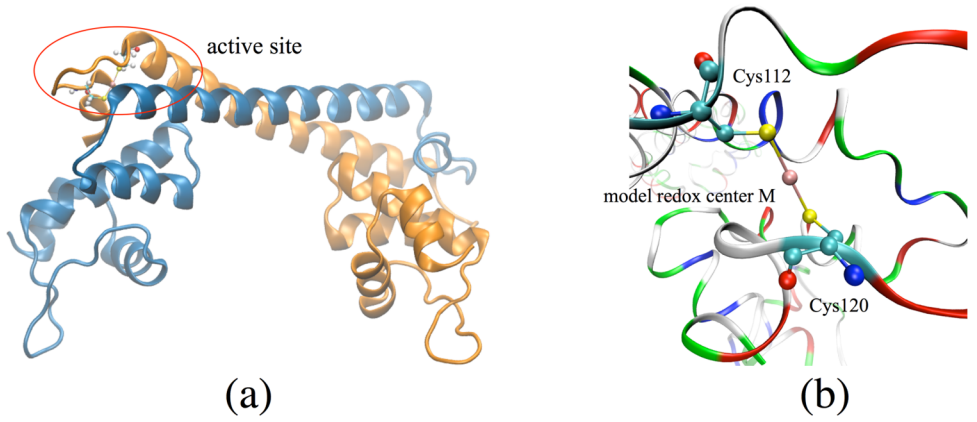

Figure 2. The CueR protein used as the model system for oxidation free energy calculations with different boundary conditions. (a) The protein is a homodimer and shown in the ribbon form. One of the metal sites is highlighted by a ellipse and the metal ion M along with its Cys ligands are shown in the ball-and-stick form. (b) A closer view of the metal site (color coding for the ribbon: red, acidic; blue, basic; green, polar; white, nonpolar). A bonded model is parametrized for the metal and its two Cys ligands. Three oxidation states of the metal site are studied, the reduced state (λ = 0, partial charge of M is +0.1158 e), the oxidized state (λ = 1, partial charge of M is +1.1158 e) and the doubly oxidized state (λ = 2, partial charge of M is +2.1158 e).

COMPUTATIONAL METHODS

Charging Free Energy of Ions in Solution. As an important benchmark and reference,[27−36] we first study the charging free energy of ions in solution using PBC and GSBP. Three common ions are chosen, Na^+, K^+, and Cl^-. The Lennard-Jones (LJ) parameters for these ions are taken from the CHARMM22 force field.[50] As to the water molecules, they are described with the modified TIP3P model in CHARMM[50,51] (simply referred to as the TIP3P model below); we also carry out a few simulations with the SPC water model.[52] Moreover, to test the "type C" correction for PME based charging free energy simulations discussed in ref 36 (see discussions in Results and Discussions), which depends on the sign of the trace of the quadrupole moment of water, we also study the charging free energy of ions in "charge reversed" water, in which the partial charges on the water oxygen and hydrogen adopt the opposite sign (i.e., oxygen with +0.834 e and hydrogen with −0.417 e).

In the PBC simulations, an ion is solvated by 1,014 water molecules in a 31.5 Å cubic box with the density of 1.0 g/cm^3. The box dimensions and temperature are controlled with MD simulations in the NPT ensemble;[4,53] the temperature is 300 K and pressure is 1 bar. Electrostatic interactions are treated with PME,[54] and the van der Waals interactions are treated with a cutoff scheme with the switch function turned on between 10 and 12 Å. The PME parameters used are κ = 0.33, B-spline interpolation order of 6, and 32 grid points for the charge mesh.

In the GSBP simulations, the system is set up with an inner region of a specific radius (8, 20, or 25 Å). Because a 2 Å buffer region is required by the smooth boundary condition between the explicit solvents and the bulk dielectric continuum, GSBP simulations with a 8/20/25 Å inner region contains a water droplet of radius 6/18/23 Å. All molecules are located in the inner region, and the outer region is described with a constant dielectric continuum with ε_w = 80. To be consistent with the GSBP protocol, electrostatic interactions among inner region atoms are treated with the extended electrostatic model[55] in which interactions beyond 12 Å are modeled with multipolar expansions, including the dipolar and quadrupolar terms. The reaction field matrix **M** is evaluated using 400/900/961 spherical harmonics for GSBP simulations with a 8/20/25 Å inner region. Temperature is controlled by coupling the system to the Nosé-Hoover thermostat[4,56,57] at 300 K.

In both boundary setups, the charging ion is fixed at the center of the box/droplet and all bonds involving hydrogen are constrained with the SHAKE algorithm,[58] allowing a 1 fs time step for MD propagation. As mentioned in the Introduction, the charging free energy is computed with a LRA protocol[59] by running MD simulations with the charge of the ion either fully turned on (λ = 0) or turned off (λ = 1). The charging free energy is then calculated as $\Delta G = 1/2(\langle q_I\Phi(0)\rangle_{\lambda=0} + \langle q_I\Phi(0)\rangle_{\lambda=1})$, where q_I is the charge (±1) of the ion and $\Phi(0)$ is the electrostatic potential at the position of the ion; the quantity $q_I\Phi(0)$ is also referred to as the "energy gap" in the following discussions. The free energy derivatives are calculated until convergence is reached for each window after an initial equilibration period of 500 ps; statistical errors are estimated by block average.[4] For correction terms for the charging free energies associated with PBC and GSBP simulations, see Charging Free Energy of Ions in a Water Droplet: Correction Terms for PME and GSBP Simulations section.

In the actual calculations, instead of computing $\Phi(0)$ explicitly, we compute the energy gap directly in CHARMM by two energy calls for each configuration with different charges for the charging ion. With GSBP,[13] for example,

$$\Delta U_{GSBP} = \left[\sum_{\alpha\in inner} q_\alpha \phi^{(o)}(\mathbf{r}_\alpha) + U^{(ii)}_{elec} + \frac{1}{2}\sum_{mn} Q_m M_{mn} Q_n\right]_{q_I=1-q_I=0} \quad (1)$$

here $\phi^{(o)}(\mathbf{r}_\alpha)$ is the electrostatic potential at $\mathbf{r}_\alpha$ due to outer region atoms, $U^{(ii)}_{elec}$ is the electrostatic interaction among inner region atoms, Q_m is the generalized multipole moment, $Q_m = \sum_{\alpha\in inner} q_\alpha b_m(\mathbf{r}_\alpha)$, and **M** is the reaction field matrix spanned by the basis functions $b_m(\mathbf{r}_\alpha)$. Although contributions from q_I to the first two terms in eq 1 are apparent, the contribution through the reaction field term is slightly more complex; q_I interacts with the reaction field due to all charges in the inner region, while other inner region charges also interact with the reaction field due to q_I.

dx.doi.org/10.1021/jp309877z | J. Phys. Chem. B 2013, 117, 2005−2018

Oxidation Free Energy for a Metal Site in a Protein. To study oxidation potential in a protein, we have chosen a somewhat unconventional model system: the metal site in a copper chaperone protein, CueR. CueR is a transcription regulator that responds to the binding of Cu(I) ion;[60−62] it is *not* known to be a redox active protein. Nevertheless, we chose it as a model system because its metal site has a similar distance from the protein/solvent boundary as blue copper proteins, which are well studied redox systems.[40,41] Compared to the blue copper proteins, CueR is larger in size and likely more flexible due to its structural topology; therefore, CueR is better suited for comparing PBC and GSBP simulations, such as probing the effect of constraining the position of protein atoms far (>20 Å) from the redox site.

The enzyme model is constructed based on the crystal structure,[60] and a bonded model is parametrized for the metal ion M, where M-ligand coordination interactions are modeled as covalent bonds and active site structural features are maintained by applying bond, angle and dihedral terms to the metal ion and its immediate ligands (Figure 2). For the purpose of this work, only the partial charge of the metal ion is changed in the "oxidation free energy" calculations; it is changed from +0.1158 e (λ = 0, the "reduced" state) to +1.1158 e (λ = 1, the "oxidized" state) and then to +2.1158 e (λ = 2, the "doubly-oxidized" state). Similar to the charging free energy of ions in solution, the oxidation free energies in CueR are calculated using the LRA protocol by running MD simulations at λ = 0, 1 and 2; energy gaps are then collected from those trajectories and then averaged to obtain the two oxidation free energies: $\Delta G = 1/2(\langle \Delta q_I \Phi(0)\rangle_{\lambda=0} + \langle \Delta q_I \Phi(0)\rangle_{\lambda=1})$, where Δq_I is the charge difference between the oxidized and reduced states of the metal ion M and $\Phi(0)$ is the electrostatic potential at M. Previous studies of reduction potential/pK_a in proteins suggested that LRA may not always apply to protein systems.[42] In our calculations, we have carefully monitored the distribution of the energy gaps and found that they closely follow Gaussian statistics in all three λ windows (see Supporting Information), suggesting that LRA is a decent approximation; we have also carried out simulations for multiple λ windows for two representative types of PBC simulations (rigid protein and fully flexible protein) to evaluate the validity of LRA for the systems studied here (see Supporting Information).

In the PBC simulations, water molecules are added to solvate the protein and the final system is a rectangular unit cell with dimensions of 64 Å × 64 Å × 120 Å; it contains 4022 protein atoms and 15 907 TIP3P water molecules. Sodium and chloride ions are added to reach a concentration of ∼0.15 M and to neutralize the total charge of the system. To better compare PBC and GSBP simulations, in addition to PBC simulations with a fully flexible protein, PBC simulations are also carried out with either the entire or part of the protein fixed; the water molecules are fully mobile in all PBC simulations. The fully rigid PBC simulations are compared to GSBP simulations with also a rigid protein; such a comparison eliminates errors that originate from sampling different protein conformations in the PBC and GSBP simulations. In PBC simulations with a partially rigid protein, the same set of atoms as in the outer region of the GSBP setup are fixed; with atoms beyond 20 (8) Å of the metal site fixed, 1021 (146) protein atoms are left fully flexible. Isothermal−isobaric ensemble is used when the entire protein is flexible; NVT ensemble is used when either the entire or part of the protein is fixed.

In the GSBP setup, the protein is partitioned into a spherical inner region (with a radius of 8 or 20 Å) while the remaining portion of the system is in the outer region, and only atoms in the inner region undergo microscopic dynamics. Protein atoms in the outer region are fixed. For the inner region of 20 Å, the initial structure for all λ windows is an equilibrated structure from the PBC simulation for a fully flexible CueR in the λ = 0 charge state; water molecules are added by superimposing the system with a water droplet of 18 Å radius centered at M and removing water molecules with oxygen atom within 2.8 Å from any heavy atoms in the initial structure. For the inner region of 8 Å, initial protein structure of each λ is taken from PBC simulation with the corresponding charge state and a fully flexible protein; the number of explicit water molecules in the GSBP simulations are determined from the average number of waters located within the 6 Å droplet centered at M in the PBC simulations. In all GSBP simulations, the protein dielectric constant is ε_p = 1, the water dielectric constant is 80; no salt concentration is considered, although test calculations indicate that including 0.15 M of salt in the Poisson−Boltzmann (PB) calculations has very small effects. The extended electrostatic model is used to treat the electrostatic interactions among inner region atoms as described above. The reaction field matrix **M** is evaluated using 289/49 spherical harmonics for GSBP simulations with a 20/8 Å inner region. Nosé-Hoover thermostat is used to control the temperature at 300 K.

With both boundary conditions, the CHARMM22 force field[50] is used for protein residues except for the metal ion M and its Cys ligands, which are parametrized based on cluster DFT calculations (Yang, S.;Cui, Q., unpublished results). During all MD simulations, all bonds involving hydrogen are constrained with the SHAKE algorithm,[58] and the time step is set as 1 fs. All simulations are equilibrated for 500 ps and then sampled for 3−9 ns, depending on the flexibility of protein. In all free energy derivatives calculations, atoms that are bound to the metal ion M are also treated as point charges (using the NBXMOD command in CHARMM); this facilitates the comparison with analysis using PB calculations (see below).

Analysis of Differences between PBC and GSBP Simulations. As discussed in greater detail in the next section, PBC (PME) and GSBP free energy results differ substantially in numerical values for both solution and enzyme (CueR) cases. Qualitatively, this is understood in terms of several corrections necessary for both types of simulations (see Figure 1). For GSBP, the correction is mainly related to the polarization of water molecules at the boundary of the finite sphere, although the smooth dielectric boundary approximation is also shown below to require extra care when the inner region is highly charged. For PME, the largest correction observed in this work (using the PME implemented in CHARMM[63]) is due to the use of particle-based summation scheme in computing electrostatic potential at the site of interest.[49] To understand these corrections more quantitatively, we analyze electrostatic potentials in the systems of interest using PB calculations with the PBEQ module in CHARMM.[64]

Analysis of Electrostatic Potential in a Spherical Water Droplet. To understand the difference between PBC and GSBP for the charging free energy in solution, we analyze the average electrostatic potentials in three types of spherical water droplets at 300 K: a droplet with the orientation disorder limit (ODL) ensemble,[36] a droplet with GSBP and a droplet with vacuum beyond the boundary. A quartic restraining potential is applied to water molecules in all setups: $V_{geo}(r)$ =

dx.doi.org/10.1021/jp309877z | J. Phys. Chem. B 2013, 117, 2005−2018

Table 1. Uncorrected Charging Free Energy (in kcal·mol^{-1}) Calculated Using PBC and GSBP Boundary Conditions[a]

water model and ion type	PBC (32 Å)[b]	GSBP (20 Å)[c]	$\Delta G_{PBC,GSBP}$
TIP3 water[d] + Na^+	−97.9 (0.6)[f]	−107.7 (0.6)/−105.1[g]	9.8 (0.8)
TIP3 water + Cl^-	−100.4 (0.7)	−91.8 (0.6)	−8.6 (0.9)
SPC water + Na^+	−96.5 (0.7)/−97.3[h]	−107.9 (0.7)	11.4 (1.0)
"Charge-reversed water"[e] + Na^+	−176.6 (0.7)	−165.9 (0.7)	−10.7 (1.0)
"Charge-reversed water" + Cl^-	−59.5 (0.4)	−68.6 (0.8)	9.1 (0.9)

[a]The uncorrected values are obtained by directly integrating the computed free energy derivatives from CHARMM simulations. As discussed in the text, the PBC results need to be revised with a "type C" correction due to the use of particle based summation scheme in PME (ΔG_{P-M}), and GSBP results need to be supplemented with a surface polarization correction (ΔG_{s-pol}). These corrections are summarized in Table 2. [b]Cubic box length for PBC simulations. [c]Radius of inner region for GSBP simulations. [d]Modified TIP3P water model in CHARMM. [e]Reverse the charges on the TIP3P water model, so that the oxygen is +0.834 e and the hydrogen is −0.417 e. [f]The values in parentheses are statistical errors based on block average. [g]Numbers before and after slash are, respectively, from this work and ref 66 which used SSBP to compute the Na^+ charging free energy in a droplet of 100 water molecules. [h]Numbers before and after slash are, respectively, from this work and ref 27.

$k_{geo} \times (r - \delta r_{off})^2 \times ((r - \delta r_{off})^2 - P_1) + k_{geo}P_1^2/4$ for $-(P_1/2)^{1/2} \le (r - \delta r_{off}) \le (P_1/2)^{1/2}$, where k_{geo} = 0.5 kcal·mol^{-1}·Å^{-1}, P_1 = 2.25 Å^2 and the offset distance δr_{off} is 15.5 Å. The ODL ensemble refers to a water simulation in the absence of electrostatic interactions; charges are put back for the analysis of electrostatic potentials. Both TIP3P and SPC water models are tested because TIP3P is widely used together with the CHARMM force field, and SPC was used in the original analysis of Hünenberger and co-workers.[8,36,49] In all droplet simulations, the radius is 18 Å and the droplet consists of 748 water molecules. The extended electrostatic model is used to approximate exact Coulomb interactions without any cutoff. Each simulation runs for 1 ns and the last 1000 snapshots (500 ps) are used for analysis. To evaluate the electrostatic potential distribution in the sphere, 10 000 sites are chosen randomly in each configuration; electrostatic potential due to all solvent charges at each site is calculated by averaging over all the grid points inside a 1 Å^3 cubic box using the PBEQ module[64] in CHARMM.

Poisson−Boltzmann Analysis for the Smooth Dielectric Boundary in GSBP. To better understand the errors that arise from the smooth boundary approximation in GSBP (see discussions in Results and Discussions), we re-evaluate the energy gap of selected number of snapshots from GSBP simulations using PB calculations; for each snapshot, this involves two PB calculations that evaluate the direct solvent contributions and reaction field contribution from the charging ion, respectively. In the PB calculations, all explicit water molecules are retained and regarded as part of the solute, which is assigned to a dielectric constant of 1; the implicit bulk solvent has a dielectric constant of 80. The optimized radii of Nina et al.[65] based on experimental solvation free energies of small molecules are employed to determine the van der Waals surface of the microscopic solute region. Solvent−solute dielectric boundary is determined by expanding beyond the van der Waals surface with a solvent probing radius; three values (0.8, 1.4, and 2.0 Å) have been tested here. To contrast with the rough molecular surface, PB calculations with a smooth dielectric boundary (the "droplet" option in PBEQ) have also been carried out.

RESULTS AND DISCUSSIONS

Charging Free Energy of Ions in a Water Droplet: Correction Terms for PME and GSBP Simulations. The calculated charging free energy for Na^+ and Cl^- using different boundary conditions and water models are given in Table 1. With the TIP3P water model, the PBC results are comparable with those of Hummer et al,[27] who used slightly different LJ parameters for the ion and SPC water; although only data for 30 Å box are shown, the results show very little box-size dependence when a larger box (60 Å) or smaller boxes are used (data not shown). The GSBP results are consistent with those obtained with the spherical solvent boundary potential (SSBP).[66] However, there is a substantial difference of approximately ±10 kcal/mol between PBC and GSBP results for a specific type of ion: GSBP overestimates the charging free energy of Na^+ but underestimates the value for Cl^-. This is not due to the difference in the solvation structure of the ions, as the ion−water oxygen radial distribution functions calculated from PBC and GSBP are practically identical for both Na^+ and Cl^- (data not shown). Rather, the difference is due to corrections needed for the treatment of electrostatics in GSBP and PBC simulations.

According to Kastenholz et al.,[49] two types of corrections are relevant to the simulations considered here (see Figure 1). The first is the P-M type correction (referred to as type C_1 correction in ref.[49]), which accounts for (a nearly constant) the difference in the electrostatic potential computed by summation in the particle (P) and molecular (M) schemes. It was argued that the M scheme is more physical;[49] for example, in an orientation disorder limit (ODL), the P scheme leads to an incorrect net external potential in the water droplet while the M scheme does not. Since the P scheme is used in PME, while the M scheme is used for GSBP (group based cutoff with extended electrostatics), the P-M correction needs to be considered when comparing PBC and GSBP charging free energies. The magnitude of the P-M correction can be estimated in two ways: (i) an analytical expression for the correction electrostatic potential, $\Delta\Phi_{ODL}^{anal} = (6\varepsilon_0)^{-1}\rho\gamma$, which was derived based on an isotropic quadrupole (IQ) liquid;[36] ε_0 is the vacuum dielectric permittivity, ρ the liquid number density and γ the trace of the quadrupole moment of the water model. (ii) Numerically evaluate the average electrostatic potential or external electrostatic potential (potential at a site that is not too close to any atom in the solvents) of the ODL water ensemble, $\Delta\Phi_{ODL}^{numr}$. The $\Delta\Phi_{ODL}^{anal}$ is 17.8 kcal·mol^{-1}·e^{-1} for the TIP3P water model and 19.1 kcal·mol^{-1}·e^{-1} for SPC, while $\Delta\Phi_{ODL}^{numr}$ is 12.4 kcal·mol^{-1}·e^{-1} for TIP3P and 17.8 kcal·mol^{-1}·e^{-1} for SPC (Table 2). Since the IQ liquid deviates from "real" water models, the analytical value $\Delta\Phi_{ODL}^{anal}$ may not be quantitatively appropriate for realistic simulations, we chose the second option to calculate the P-M correction required for the charging free energy; this takes the form of $\Delta G_{P-M} = -\Delta q_I \Delta\Phi_{ODL}^{numr}$ and is needed for the PBC result.

dx.doi.org/10.1021/jp309877z | J. Phys. Chem. B 2013, 117, 2005−2018

Table 2. The Average Potential (in kcal·mol^{-1}·e^{-1}) in Spherical Water Droplets and the Derived Correction Terms for PME/GSBP Charging Free Energy Simulations

finite size boundary condition	average potential[a]
ODL[b]	−12.4/−12.4/−17.8/−16.8
GSBP[c]	−10.5/−11.0/−12.6/—
Vacuum[d]	−10.3/−11.0/−12.4/−13.7
ΔG_{P-M}[e]	−12.4/−12.4/−17.8/−16.8
ΔG_{s-pol}[f]	−1.9/−1.4/−5.2/—

[a]For each entry, the numbers are calculated based on the modified TIP3P water model in an 18 Å water droplet, the modified TIP3P water model in a 23 Å water droplet, the SPC water model in an 18 Å water droplet; the last value, when available, is from ref 36 which used the SPC water model and a Lennard-Jones boundary potential instead of the quartic boundary potential used here. [b]ODL refers to the orientation disorder limit ensemble[36] (simulations in the absence of electrostatic interactions) with a quartic boundary potential (see text). [c]The outer region of GSBP is the dielectric continuum with ε = 80; water molecules near the interface are subject to the same quartic boundary potential. [d]The water droplet is surround by vacuum; water molecules near the interface are subject to the same quartic boundary potential. [e]The P-M correction for the PME charging free energy[36,49] calculated based on the average electrostatic potentials from the ODL ensemble. [f]The surface polarization correction for GSBP charging free energy calculated based on the difference in the average potential between ODL and GSBP simulations.

The second correction is a surface (fluid-continuum interface) polarization contribution (referred to as the type C_2 correction in ref 49), which accounts for the spurious anisotropy of water molecules close to the boundary of finite sphere simulations. This is illustrated explicitly in Figure 3,

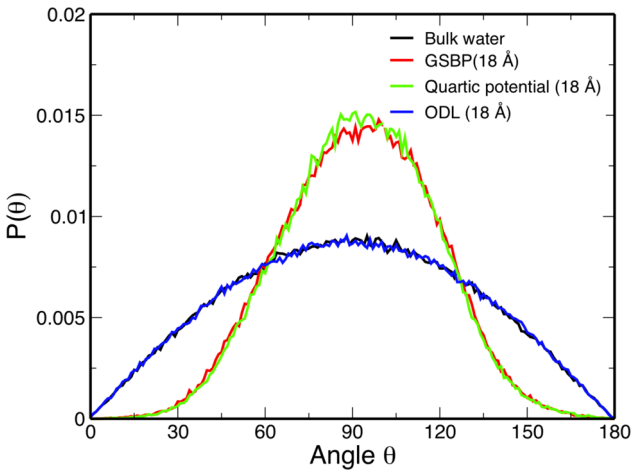

Figure 3. The orientation distribution of water molecules in bulk (based on PBC calculations), an ODL ensemble and two other water droplet simulations; for the last three cases, orientations for water molecules within 1.5 Å from the droplet surface are shown. The orientation is defined as the angle between the water dipole and the normal vector of the local surface.

which plots the orientational distribution (between the water dipole and surface normal of the droplet) for water molecules within 1.5 Å from the boundary. Clearly, the surface water molecules in GSBP have a preferential orientation compared with bulk water or the ODL ensemble, and this leads to an increase of electrostatic potential at the charging ion; the magnitude of the polarization is similar when a water droplet is placed in vacuum (with the same radial quartic potential applied to the surface water) instead of a dielectric continuum of ε = 80 in GSBP. We evaluate the effect due to this artificial polarization by taking the difference of the average electrostatic potential inside a water droplet sampled with regular GSBP and an ODL ensemble; the corresponding correction to the charging free energy is then, $\Delta G_{s-pol} = -\Delta q_I \Delta\Phi_{surf}$, and needs to be added to the GSBP result.

As shown in Table 2, the average potential in a 18 Å water droplet sampled with ODL and GSBP using the TIP3P model is −12.4 kcal·mol^{-1}·e^{-1} and −10.5 kcal·mol^{-1}·e^{-1}, respectively. These imply that, for the charging free energy of a cation, the P-M correction (ΔG_{P-M}) is −12.4 kcal/mol and the surface polarization correction (ΔG_{s-pol}) is −1.9 kcal/mol. Including these corrections to the uncorrected PBC and GSBP results summarized in Table 1 leads to consistent charging free energies for Na^+ as −110.3 kcal/mol with PBC and −109.6 kcal/mol with GSBP. Alternatively speaking, the difference of −10.5 kcal/mol between the P-M correction and surface polarization correction explains the difference between uncorrected PBC and GSBP charging free energies for Na^+. Moreover, since both ΔG_{P-M} and ΔG_{s-pol} depend linearly on the sign of the charging ion (q_I), their values as well as the difference between them adopt the opposite sign when considering the charging free energy of an anion; this is consistent with the observation noted above (Table 1) that uncorrected GSBP result is lower than the uncorrected PBC result for Cl^- by approximately +10 kcal/mol. Similar electrostatic potentials are also computed for a larger water droplet with a radius of 23 Å (Table 2), suggesting that the potentials are insensitive to the droplet size for GSBP or SSBP simulations.

As a further validation, we examine the charging free energies of Na^+ and Cl^- in a "charge-reversed" TIP3P water droplet (private communication with Gabriel Rocklin). In the charge-reversed water model, the partial charges on oxygen and hydrogen are inverted from those in the standard TIP3P model; that is, oxygen has +0.834 e and hydrogen has −0.417 e. Because of the pairwise additive nature of a classical Coulomb model, inverting the partial charges does not change the water−water interactions. However, the charge inversion flips the sign of the quadrupole trace of the water model and therefore the sign of both ΔG_{P-M} and ΔG_{s-pol} for charging free energy calculations. Indeed, as shown in Table 1, the difference between uncorrected GSBP and PBC charging free energies in "charge-reversed" water is of the same absolute magnitude as with the TIP3P model for a specific ion, albeit with the opposite sign.

With the SPC model, the average potential in an 18 Å water droplet sampled with an ODL ensemble and a radial quartic restraining potential is −17.8 kcal·mol^{-1}·e^{-1} and −12.4 kcal·mol^{-1}·e^{-1}, respectively; these are in good agreement with values reported in ref 49 despite that a L-J restraining potential was used for surface water molecules. Accordingly, the expected difference between uncorrected PBC and GSBP charging free energies for a cation in SPC water is about −12.6 kcal/mol, which is close to the computed values of 11.4 kcal/mol for Na^+ (see Table 1).

Finally, since both ΔG_{P-M} and ΔG_{s-pol} do not depend on the characteristics of the ion other than its charge, we expect that they cancel out for the relative charging free energy of ions of the same charge. Indeed, as shown in Table 3, GSBP and PBC

dx.doi.org/10.1021/jp309877z | J. Phys. Chem. B 2013, 117, 2005−2018

give very consistent relative charging free energy for Na^+ and K^+, even for GSBP calculations with a small radius (8 Å).

Table 3. Relative Charging Free Energy for Cations (in kcal·mol^{-1}) Calculated Using PBC and GSBP Boundary Conditions

boundary condition	Na^+	K^+	$\Delta G_{Na^+,K^+}$
PBC (32 Å[a])	−97.9 (0.6[c])	−77.3 (0.5)	−20.6 (0.8)
GSBP (25 Å[b])	−107.7 (0.5)	−87.1 (0.5)	−20.6 (0.7)
GSBP (20 Å[b])	−107.7 (0.6)	−86.8 (0.6)	−20.9 (0.8)
GSBP (8 Å[b])	−108.9 (0.6)	−89.1 (0.7)	−19.8 (0.9)

[a]Cubic box length for PBC simulations. [b]Radius of inner region for GSBP simulations. [c]The values in parentheses are statistical errors based on block average.

Charging Free Energy of Na^+ in a Water Droplet with Additional Charges: Smooth Boundary in GSBP Simulations. As discussed below, GSBP appears to be problematic when dealing with an inner region that has a high net charge. To better understand the situation, we study the charging free energy of Na^+ in water in the presence of several (1−5) Cl^- ions with both PBC and GSBP simulations. As shown in Table 4, the PBC results do not vary much at all with up to 5 Cl^- in a 30 Å box; the uncorrected value remains close to −98.0 kcal/mol. By contrast, the uncorrected GSBP result steadily increases from −107.7 to −116.7 kcal/mol as the number of Cl^- increases from 0 to 5. As a result, the difference between uncorrected GSBP and PBC results significantly increases from 9.8 to 18.2 kcal/mol as the number of Cl^- increases to 5.

Qualitatively, we believe that this additional problem for GSBP is due to the fact that the uncertainty associated with computing electrostatic solvation free energy using the smooth dielectric boundary approximation in GSBP becomes increasingly large as the inner region charge increases. For the charging free energy of a cation in a water droplet, the dominant GSBP contribution is the Born term associated with the net charge of the inner region: $(Q + 1)^2/2R_{in} - Q^2/2R_{in} = (2Q + 1)/2R_{in}$, where Q is the charge of the inner region without considering the charging ion and R_{in} is the effective size of the inner region. Clearly, this term becomes large when Q is large; similarly, any uncertainty in the estimation of R_{in} would also lead to a significant error in the GSBP contribution when Q is large.

To circumvent the problem, we re-evaluate the energy gaps from selected (1000) snapshots from GSBP simulations using PB calculations; the free energy derivatives are corrected by taking the difference between PB and GSBP energy gaps for these snapshots.The use of exact PB solution with a detailed dielectric boundary to postprocess the MD conformations was also used by Simonson in previous work.[43] As shown in Table 4, this works very well. For example, with the typically recommended value for the solvent probe radius of 1.4 Å, the PB-corrected GSBP charging free energy for Na^+ in the presence of 5 Cl^- becomes −109.0 kcal/mol, which is close to the value of −107.7 kcal/mol without any Cl^-; the standard deviation for the PB correction among the 1000 snapshots is about 0.7 kcal/mol (for more details, see Supporting Information). The PB correction is fairly insensitive to the solvent probe radius. With a smooth dielectric boundary of radius 20 Å, which is the same as in the GSBP setup, however, the PB correction is essentially zero, further confirming that the underlying problem is due to the uncertainty associated with computing electrostatic solvation free energy using a smooth dielectric boundary. Therefore, for charging free energy simulations with GSBP, extra care needs to be exercised when the inner region is highly charged; one effective way to circumvent the problem is to perform PB corrections based on selected snapshots.[43] This is found effective for both solution and protein (see below) systems.

Oxidation Free Energy for the Metal Site in a Fixed CueR Protein. To better explore the impact of the issues discussed above on GSBP and PBC charging free energy calculations for proteins, we first discuss oxidation free energy calculations for a metal site in a fixed CueR system. In this way, we avoid contributions due to differences in the sampled configurations in GSBP and PBC simulations; these contributions will be discussed in the next subsection.

As shown in Table 5, similar to the situation of charging free energy in a water droplet, GSBP and PBC calculations give very consistent results for the relative oxidation free energy for two metal sites that differ by the size of the metal ion. The van der Waals radius of the metal ion is taken to be 1.68 and 0.68 Å, respectively, and the relative oxidation free energy is 11.5 and 10.9 kcal/mol for PBC and GSBP, respectively. The basic

Table 4. Calculated Charging Free Energy (in kcal·mol^{-1}) of Na^+ with Different Net Charges in the Systems Using PBC and GSBP Boundary Conditions, and Poisson-Boltzmann Correction for the GSBP Results

net charge[a]	PBC (32 Å[b])	GSBP (20 Å[c])	$\Delta G_{PBC,GSBP}$
0	−97.9 (0.6)[d]	−107.7 (0.6)	9.8 (0.8)
−1	−98.0 (0.6)	−109.3 (0.6)	11.3 (0.8)
−2	−97.9 (0.5)	−110.9 (0.7)	13.0 (0.9)
−3	−98.4 (0.8)	−113.1 (0.5)	14.7 (0.9)
−4	−98.2 (0.7)	−115.3 (0.4)	17.1 (0.8)
−5	−98.5 (0.6)	−116.7 (0.6)	18.2 (0.8)
solvent probe radii	PBC (32 Å)	PB[e]	difference
0.8 Å/1.4 Å/2.0 Å	−98.5 (0.6)	−110.6/-109.0/-109.0 (0.8)	12.1/10.5/10.5 (1.0)
20 Å droplet[f]	−98.5 (0.6)	−117.0 (0.8)	18.5 (1.0)

[a]Different numbers of Cl^- are added to the system to adjust the total net charge; a neutral sodium atom is taken as the reference to specify the net charge of the system. [b]Cubic box length for PBC simulations. [c]Radius of inner region for GSBP simulations. [d]The values in parentheses are statistical errors based on block average. [e]Snapshots used in PB calculations are taken from GSBP simulations with −5 net charge; the dielectric constant is set to 1 for all explicit solvent/ions and 80 for the bulk (continuum) solvent. [f]A smooth dielectric boundary condition with a radius of 20 Å (ε = 1) is used to mimic the GSBP setup.

dx.doi.org/10.1021/jp309877z | J. Phys. Chem. B 2013, 117, 2005−2018

Table 5. Oxidation Free Energy (in kcal·mol^{-1}) for a Metal Site M in a Rigid CueR Protein Calculated Using PBC and GSBP Boundary Conditions

boundary condition	M[a]	M′[b]	$\Delta G_{M,M'}$
PBC	−74.5 (1.2[c])	−86.0 (1.3)	11.5 (1.8)
GSBP (20 Å)	−99.6 (0.9)	−110.5 (1.2)	10.9 (1.5)

[a]M is the model redox center in CueR with a van der Waals radius of 1.68 Å. [b]M is the model redox center in CueR with a smaller van der Waals radius of 0.68 Å. [c]The values in parentheses are statistical errors based on block average.

trends can be understood by looking at the water accessibility of the metal site. As shown in Figure 4, the metal site is not immediately accessible to water in the "reduced state" (q_I = +0.1158e, λ = 0) regardless of the van der Waals radius of the metal ion or the boundary condition; this is expected because the partial charges and bonded parameters of the "reduced" metal ion are developed to reflect the buried nature of the metal site in CueR.[60] In the "oxidized state" (q_I = +1.1158e, λ = 1), the metal site becomes more water accessible as indicated by the significant water distribution peak at fairly short metal−oxygen distances (<3 Å), especially for the metal ion with the smaller van der Waals radius (Figure 4d). For all the states sampled, GSBP and PBC give essentially identical water distributions around the metal site.

For a specific metal ion, however, the PBC and GSBP oxidation free energies (without the corrections discussed in the last two subsections) differ by as much as 25 kcal/mol, which is significantly different from the value of ∼10 kcal/mol found for charging free energies in solution. The discussion below suggests that this deviation is due to the high charge of the inner region in the GSBP simulations of CueR. Indeed, with a sphere of 20 Å that centers on the metal site, the inner region has a charge of −8.12 e, leaving the outer region with a charge of −3.88 e; these charges are not integers because the smooth dielectric boundary is determined by geometry instead of using a group-based criterion. Perturbative analyses are then performed to better understand the role of these net charges on the calculated oxidation free energy; the net charges are modulated by applying the neutralized (not zero) partial charge models for charged residues[67] to selected residues or, as an extreme model, setting all partial charges of protein residues to zero.

As seen in Table 6, the calculated oxidation free energy using PBC (∼75 kcal/mol) is in fact fairly insensitive to these charge perturbations to either the inner or outer regions, unless the immediate ligands of the metal ion (Cys112 and Cys120) are also set to zero (leading to a net charge of −0.12 e for the inner

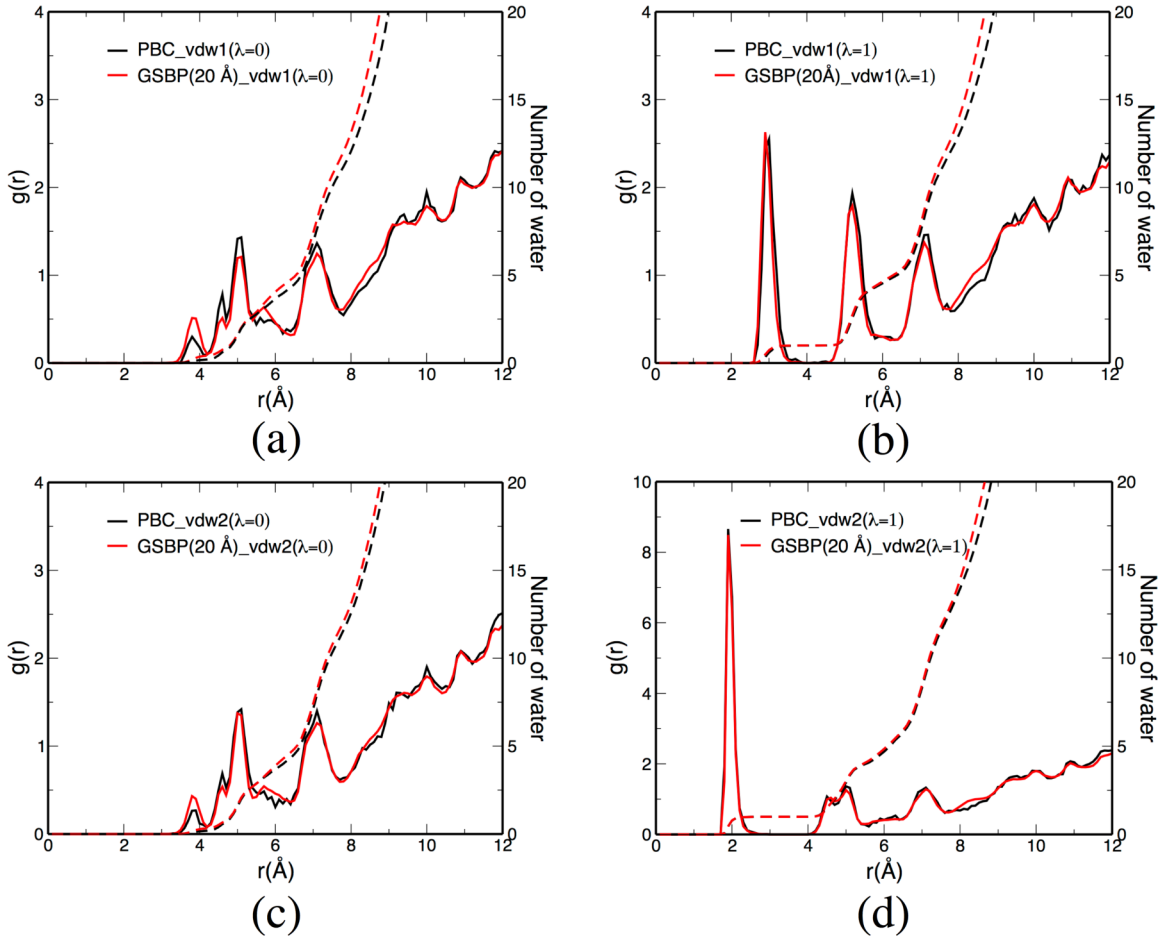

Figure 4. Radial distribution function of water oxygen around M in PBC and GSBP (20 Å) simulations of a rigid CueR protein. Different boundary conditions give reasonably similar water distributions. (a) M in the reduced state (λ = 0) with a van der Waals radius of 1.68 Å; (b) M in the oxidized state (λ = 1) with a van der Waals radius of 1.68 Å; (c) M in the reduced state (λ = 0) with a van der Waals radius of 0.68 Å; (d) M in the oxidized state (λ = 1) with a van der Waals radius of 0.68 Å.

dx.doi.org/10.1021/jp309877z | J. Phys. Chem. B 2013, 117, 2005−2018

Table 6. Oxidation Free Energy (in kcal·mol^{-1}) of a Metal Site M in a Rigid CueR Protein Calculated with Different Net Charges Using PBC and GSBP Boundary Conditions, and Poisson-Boltzmann Correction for the GSBP Results

net charge distribution[a]	PBC[b]	GSBP (20 Å)	$\Delta G_{PBC,GSBP}$
inner: −8.12, outer: −3.88[c]	−74.5 (1.2[f])	−99.6 (0.9)	25.1 (1.5)
inner: −2.12, outer: −3.88[d]	−74.6 (0.7)	−88.3 (0.6)	13.7 (0.9)
inner: −0.12, outer: −3.88[d]	−69.0 (1.0)	−81.1 (0.5)	12.1 (1.1)
inner: −8.12, outer: 0.12[d]	−75.7 (0.8)	−100.0 (0.7)	24.3 (1.1)
inner: 0.0, outer: 0.0[e]	−28.7 (0.5)	−40.5 (0.7)	11.8 (0.9)

solvent probe radii	PBC	PB[g]	difference
0.8 Å/1.4 Å/2.4 Å	−74.5 (1.2)	−85.5/−85.8/−86.0 (1.5)	11.0/11.3/11.5 (1.9)
20 Å[h] droplet	−74.5 (1.2)	−99.5 (1.5)	25.0 (1.9)

[a]Net charge adjustment is realized by neutralizing charged side chains. Numbers following "inner" and "outer" are the net charges in regions that correspond to the inner and outer partitions in the GSBP simulations. [b]PBC simulations employ the same charge sets as the corresponding GSBP simulations. [c]This net charge distribution is obtained when using the standard CHARMM22 force field; the values are not integers because the inner/outer partitioning in GSBP is done based on geometrical criteria. [d]Selected number of charged residues in the inner/outer regions are neutralized by applying the EEF1 partial charges.[67] In the third row (with an inner charge of −0.12), the ligands of the metal site are also neutralized. [e]All partial charges on the protein atoms are set to zero. [f]The values in parentheses are statistical errors. [g]Snapshots used in PB calculations are from GSBP simulations with an inner net charge of −8.12 *e* and an outer net charge of −3.88 *e*; the dielectric constant is set to 1 for all explicit solvent/protein atoms and 80 for the bulk (continuum) solvent. [h]A smooth dielectric boundary condition with a radius of 20 Å (ε = 1) is used to mimic the GSBP setup.

Table 7. Oxidation Free Energy (in kcal·mol^{-1}) of a Metal Site M in CueR Using PBC and GSBP with Different Parts of Protein Fixed and a Linear Response Model

system	ΔG (λ = 1−λ = 0)[a]	ΔG (λ = 2−λ = 1)[a]	$\Delta\Delta G_{12}$
PBC (fully flexible)	−112.7 (0.8)[h]	−255.8 (0.7)	−143.1 (1.1)
PBC (+20 Å-fixed)[b]	−113.3 (1.3)	−254.7 (1.1)	−141.4 (1.7)
PBC (+8 Å-fixed)[c]	−90.1 (0.7)	-	-
PBC (+8 Å-relaxed)[d]	−115.4 (0.6)	-	-
GSBP (20 Å)[e,f]	−132.8/−119.0 (0.7)	−271.4/−259.2 (0.7)	−138.6/−140.2 (1.0)
GSBP (8 Å)[e,g]	−128.9 (0.9)	−273.1 (0.8)	−144.2 (1.2)

[a]λ = 2 is the "doubly-oxidized" state of M with a partial charge of +2.1158 *e*, λ = 1 is the oxidized state with a partial charge of +1.1158 *e*, and λ = 0 is the reduced state with a partial charge of +0.1158 *e*. [b]Fix protein beyond 20 Å of M and all water molecules are mobile. [c]Fix protein beyond 8 Å of M and all water molecules are mobile. [d]An equilibrated structure from the oxidized state of +20 Å-fixed simulation is used as the initial structure. [e]The dielectric constant of protein in the outer region is set to 1 for all GSBP simulations. [f]For each entry, the numbers after the slash contain PB correction for the smooth dielectric boundary. [g]The initial structures are equilibrated structures from PBC simulations with the corresponding charge state of M and a fully flexible protein. [h]The values in parentheses are statistical errors based on block average.

region) or all protein residues are set to have zero partial charges. This observation suggests that electrostatic interactions are fairly screened beyond the immediate neighborhood of the metal center; this is also supported by the observation that the GSBP result is not sensitive to charge perturbations in the outer region. Once the net charge of the inner region is reduced, the GSBP calculation becomes better behaved and the difference from the PBC result (without including the P-M and surface polarization corrections) approaches the value observed for charging free energies in solution (i.e., ∼10 kcal/mol). There appears to be a small deviations (∼1 kcal/mol), however, between the PBC/GSBP difference even in the limit of a low inner region charge. For example, when all protein partial charges are set to 0, the uncorrected GSBP/PBC difference in the oxidation free energy is ∼11.8 kcal/mol, which is slightly larger than the difference in PBC/GSBP charging free energies in a water droplet. This is likely because the presence of the protein reduces the fraction of the box occupied by the solvent, thereby modifying the precise values of both ΔG_{P-M} and ΔG_{s-pol}.

As a numerical remedy for the problem associated with the high-charge of the GSBP inner region, PB calculations are carried out to re-evaluate the energy gap for selected snapshots (2000) from GSBP simulations following the protocol established in the last subsection. Similar to the situation of a water droplet, this PB correction scheme is found to be effective with a fairly small standard deviation of 0.7 kcal/mol. (For more details, see Supporting Information.) With a solvent probe radius of 1.4 Å in the PB calculations, the difference between PB corrected GSBP oxidation free energy and PBC value decreases from ∼25 kcal/mol to the expected ∼11 kcal/mol. With a smooth dielectric boundary in the PB calculations, however, the correction is essentially zero, emphasizing again the importance of carefully considering the dielectric boundary when evaluating electrostatic solvation free energy in GSBP calculations with a highly charged inner region.

Oxidation Free Energy for the Metal Site in a Flexible Protein with a LRA Model. Finally, as the most realistic example, we study the oxidation free energy of the metal site in a flexible CueR and explore how sensitive is the result to the details of the boundary condition with a LRA model.

To better compare PBC and GSBP, in addition to PBC simulations with a fully flexible protein, we also carry out PBC simulations with the region that corresponds to the outer region of a GSBP setup held fixed to the crystal structure configuration; atoms beyond 8 and 20 Å from the metal site are held fixed, and the simulations are referred to +8 Å-fixed and +20 Å-fixed PBC simulations, respectively. We first compare these three PBC simulations.

dx.doi.org/10.1021/jp309877z | J. Phys. Chem. B 2013, 117, 2005−2018

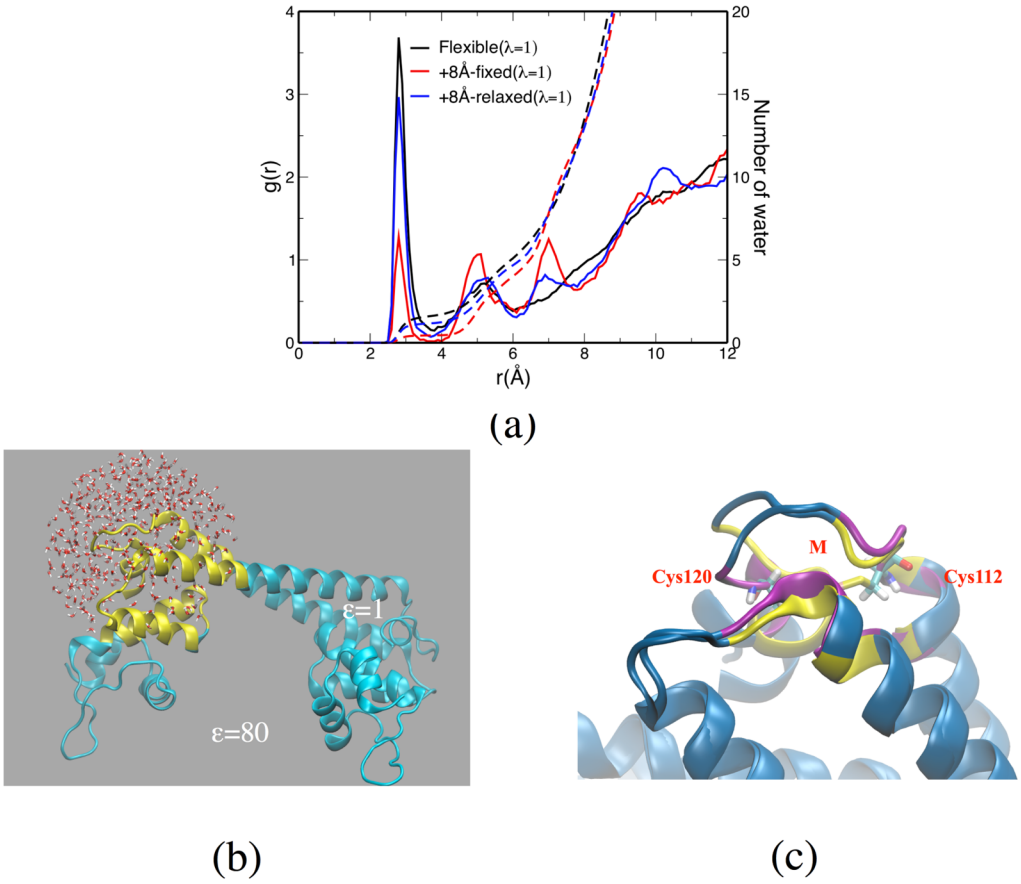

Figure 5. Properties of PBC and GSBP simulations with a partially or fully flexible CueR. (a) Radial distribution function of water oxygen around M (oxidized state, $\lambda = 1$) in PBC simulations with different parts of the CueR protein held fixed. (b) A snapshot that illustrates the GSBP (20 Å) setup; protein atoms beyond 20 Å of M are fixed (cyan), those within 20 Å of M are flexible (yellow) and the bulk continuum is indicated with a gray background. (c) Overlay of +8 Å-fixed and +8 Å-relaxed structures for the oxidize state after 1 ns production run. The flexible protein region from the +8 Å-fixed structure is shown in yellow, and that in the +8 Å-relaxed structure is shown in purple; the fixed protein region is colored in blue. Clearly, the metal binding loop responds to the metal oxidation and therefore should be allowed to relax for reliable oxidation free energy calculations (see Table 7 and text for discussion).

As shown in Table 7, the first oxidation free energies (q_I = +0.1158e, $\lambda = 0$ to q_I = +1.1158e, $\lambda = 1$) from the fully flexible and +20 Å-fixed PBC simulation are fairly similar to each other; the values are −112.7 and −113.3 kcal/mol, respectively. This suggests that the reorganization of protein atoms and water molecules within 20 Å of the metal site make the dominant contribution while the response from atoms further away is minimal due to effective screening. By contrast, the +8 Å-fixed PBC simulation (−90.1 kcal/mol) underestimates the oxidation free energy by as much as 22.5 kcal/mol, suggesting that the proper conformational response to the metal oxidation is not captured in the more restrictive +8 Å-fixed PBC setup. By comparing the protein conformation and water distribution in different oxidation states from different PBC simulations, we found that the response of the metal binding loop to the metal oxidation is too restricted in the +8 Å-fixed setup (see Figure 5c), which in turn also limits the solvent accessibility of the metal site in the oxidized ($\lambda = 1$) state; as shown in Figure 5a, on average one less water is found within the first solvation shell of the oxidized metal site in the +8 Å-fix simulation as compared to the fully flexible case.

To further quantify the importance of these conformational differences, we carry out another set of PBC simulation in which protein atoms beyond 8 Å from the metal site are also held fixed; however, the initial structures in the reduced ($\lambda = 0$) and oxidized ($\lambda = 1$) windows are taken from the equilibrated structures in the respective +20 Å-fixed simulations. We refer this new set of simulations as the +8 Å-relaxed set, which in principle should have captured most of the conformational response to metal oxidation. As shown in Table 7, the +8 Å-relaxed PBC result (−115.4 kcal/mol) is indeed much closer to the +20 Å-fixed and fully flexible PBC simulations (∼-113 kcal/mol), confirming that it is important to leave flexibility in the model so that rearrangement of nearby structural motifs (e.g., the metal binding loop) occurs without artificial hindrance; it seems, however, less important to sample the thermal fluctuation of atoms beyond 8 Å.

We now move on to GSBP simulations. The comparison of the various PBC results suggests that fixing atoms beyond 20 Å from the metal site has a small impact on the oxidation free energy. Therefore, we expect that GSBP simulations with a 20 Å inner region yield reliable results; the only difference from the +20 Å-fixed PBC simulation is the treatment of the bulk solvent and the dielectric boundary of the inner region. Without the PB correction for the smooth dielectric boundary approximation, the GSBP result with a 20 Å inner region differs from the PBC results by about 20 kcal/mol; with the PB correction included, the difference is reduced to about 6 kcal/mol, which is somewhat different from the GSBP/PBC difference observed for fixed protein simulations (∼12 kcal/

dx.doi.org/10.1021/jp309877z | J. Phys. Chem. B 2013, 117, 2005−2018

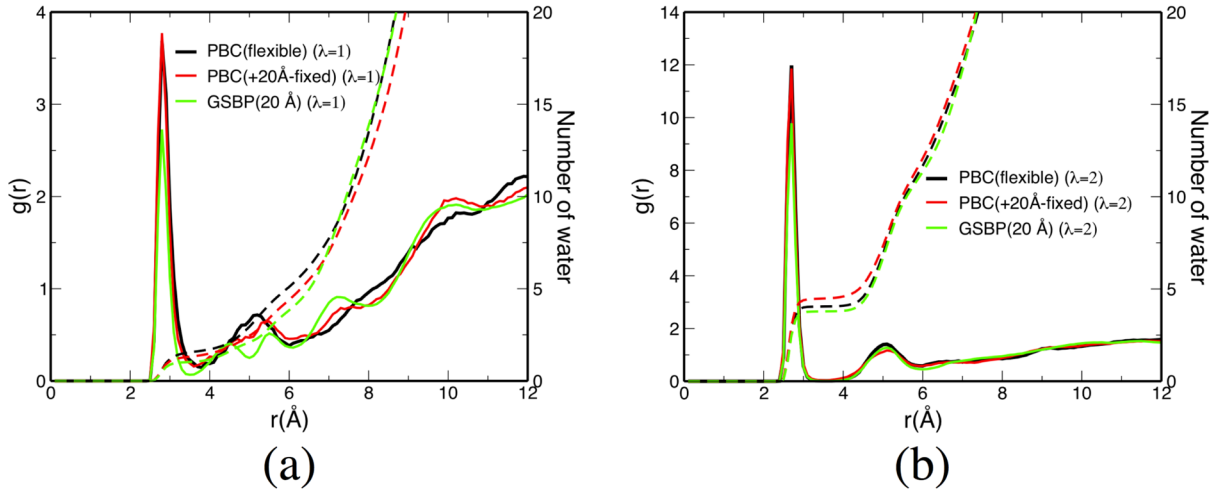

Figure 6. Radial distribution function of water oxygen around M in PBC (flexible or 20 Å-fixed) and GSBP (20 Å) simulations. (a) M in the oxidized state (λ = 1). (b) M in the doubly oxidized state (λ = 2). Different boundary conditions lead to reasonably similar water distributions.

mol, see Table 6). In other words, it appears that ΔG_{P-M} and ΔG_{s-pol} are not highly transferrable among water and protein systems.

As an additional test along this line, we compute another oxidation free energy in which the metal site is further oxidized (q_I = +2.1158e,λ = 2) and we compare the difference from the first oxidation free energy using several simulation protocols; the goal is to see to what degree ΔG_{P-M} and ΔG_{s-pol} cancel for the relative oxidation free energy, which is often the quantity of interest, in different computational protocols. As shown in Table 7, the $\Delta\Delta G_{12}$ from GSBP (20 Å) simulations after the PB dielectric boundary correction is −140.2 kcal/mol, which is reasonably close to the values from fully flexible (−143.1 kcal/mol) and +20 Å-fixed (−141.4 kcal/mol) PBC simulations; even without the PB correction, the $\Delta\Delta G_{12}$ from GSBP (20 Å) is within a few kcal/mol from the PBC results. This is consistent with the finding that solvent distributions near the metal site are similar between the GSBP and those two PBC simulations for both λ = 1 and λ = 2 windows (see Figure 6).

When a smaller inner region (8 Å) is used for GSBP, analysis of the various PBC results suggests that different structures should be used for different λ windows for reliable results. Therefore, the initial structures in GSBP (8 Å) are taken from the fully flexible PBC simulations with the corresponding charge state for the metal site. The oxidation free energies obtained from these GSBP (8 Å) simulations are −128.9 kcal/mol for $\Delta G(\lambda = 1$ to $\lambda = 0)$, −273.1 kcal/mol for $\Delta G(\lambda = 2$ to $\lambda = 1)$ and therefore a difference of −144.2 kcal/mol for $\Delta\Delta G_{12}$; this is reasonably close to the PBC and GSBP (20 Å) results. However, we note that the absolute values for the oxidation free energies from the GSBP (8 Å) simulations remain fairly different from the PBC results; as shown in Table 7, they are in fact somewhat close to the GSBP (20 Å) results without the PB correction for the smooth boundary approximation. Since the inner region of the GSBP (8 Å) simulations do not feature a significant net charge, the effect of the smooth boundary approximation is not significant; test calculations indicate a contribution in the range of 1−2 kcal/mol. Therefore, further studies are needed to elucidate the origin for the larger difference between GSBP (8 Å) and PBC results.

Nevertheless, especially for relative oxidation free energies (i.e., $\Delta\Delta G_{12}$), the GSBP simulations with ε_p = 1 for the outer region leads to good agreement with PBC simulations. This might be due to special features of CueR, which has the metal binding site fairly accessible to the solvent. As a result, the interactions with other charges in the protein are very effectively screened out. For other systems with a deeply buried redox site, a more sophisticated description for the outer region dielectrics might be required. In our study of microscopic pK_a of a deeply buried Glu residue in the transmembrane protein cytochrome c oxidase, for example, the protonation state of titratable residues within 15−20 Å range was found to make notable contributions.[19,68]

CONCLUDING REMARKS

Despite the rapid progress in computational hardware, it often remains attractive to construct computational models for biomolecules with a finite sphere boundary condition. This allows one to focus on the sampling of a fairly localized region without the need of sampling far away regions. This is clearly most advantageous when the system of interest is very large (e.g., the ribosome) and/or the potential function is expensive (e.g., ab initio QM/MM). On the other hand, it should be kept in mind that many approximations are inherent to the finite sphere boundary framework, and whether these approximations make a significant impact on the problem of interest should be evaluated with care. The most obvious issue is whether the process under study implicates collective structural changes or a significant change in the level of solvation in the active site. If so, one should either resort to PBC simulations for better conformational sampling or other specialized simulation techniques to better sample water distributions.[69,70]

In the current work, we focus on the treatment of electrostatic properties by finite sphere boundary condition and compare the results with PBC simulations; electrostatics are of special interest because they often dominate the energetics of processes that occur in biomolecules. Specifically, we compare charging free energies in both solution and protein systems calculated with GSBP and PME simulations. With a change in the net charge, the results of these free energy simulations are sensitive to various approximations and therefore particularly informative to the comparison of simulation protocols.

dx.doi.org/10.1021/jp309877z | J. Phys. Chem. B 2013, 117, 2005−2018

For simple ions in solution, we find good agreements between GSBP and PBC charging free energies, once the relevant correction terms are taken into consideration. For PBC simulations with PME for long-range electrostatics, the contribution (ΔG_{P-M}) due to the use of a particle rather than molecule based summation scheme in real space is found to be significant, which was first pointed out by Hünenberger and co-workers.[36,49] For GSBP, when the inner region is close to be charge neutral, the key correction is the over polarization of water molecules at the inner/outer dielectric boundary; the magnitude of the correction (ΔG_{s-pol}), however, is relatively minor (~2 kcal/mol with TIP3P).

For charging (oxidation) free energy in proteins, the situation is more complex although good agreement between GSBP and PBC can still be obtained when care is exercised. For example, we observe that the smooth dielectric boundary approximation inherent to GSBP tends to make significant errors when the inner region is featured with a high net charge. However, the error can be corrected with Poisson−Boltzmann calculations using snapshots from GSBP simulations in a straightforward and robust manner. Because of the more complex charge and solvent distributions, the magnitudes of ΔG_{P-M} and ΔG_{s-pol} in protein simulations appear to be different from those derived for solution simulations. Therefore, it remains somewhat challenging to directly compare absolute charging free energies in PBC and GSBP simulations for protein systems; the relative charging/oxidation free energies, however, are more robust and PBC/GSBP results agree much better even for GSBP simulations with a fairly small inner region.

For the specific protein system (CueR) studied, the use of a low-dielectric "constant" for the outer region is found to introduce only a small error to the oxidation free energy, especially when the inner region is as large as 20 Å; even with a 8 Å inner region, using a dielectric constant of 1 for the outer region leads to a relative oxidation free energy that agrees fairly well with PBC and GSBP (20 Å) simulations with a LRA model. These results are likely due to the fact that the site of interest is fairly solvent accessible and therefore well screened from the outer region. For a deeply buried site, a more sophisticated treatment for the dielectrics for the outer region[2,71] might be needed. An important benchmark for the near future, therefore, concerns oxidation/reduction or pK_a calculations in transmembrane proteins. Although several GSBP studies have been carried out for bacteriorhodopsin[19,20] and cytochrome c oxidase,[19,68] a systematic comparison to PBC simulations and multifaceted comparisons to available experimental data will be essential to establishing the quantitative accuracy (and limitation) of GSBP for membrane proteins.

Finally, with a LRA model, the effect of freezing the protein structure in the outer region is found to be small, unless a very small (8 Å) inner region is used; even in the latter case, the result becomes substantially improved when the nearby metal binding loop is allowed to respond to metal oxidation. In other words, while it is important to leave flexibility in the model so that rearrangement of nearby structural motifs in response to metal oxidation occurs without artificial hindrance, it seems less important to sample the thermal fluctuation of atoms beyond 8 Å. The quantitative validity of this observation when LRA is no longer assumed needs to be evaluated carefully; this requires very extensive conformational sampling and we are pursuing that with a realistic redox protein (plastocyanin) because its reorganization energy is substantially smaller than the one observed for CueR (see Supporting Information). Nevertheless, the observations in this work are informative to ab initio QM/MM calculations. On one hand, they highlight the importance of carrying out adequate sampling rather than limited structural minimizations. On the other hand, they support a practical approach in which one equilibrates the system using MM or semiempirical QM/MM with either PBC or large-inner-region GSBP simulations, then carries out ab initio QM/MM calculations using GSBP/SMBP[72,73] but with a smaller inner region.

■ ASSOCIATED CONTENT

Supporting Information

Additional details regarding the distribution of PB corrections for the smooth dielectric boundary approximation in GSBP and discussion of the validity of LRA for the CueR system are included. This material is available free of charge via the Internet at http://pubs.acs.org.

■ AUTHOR INFORMATION

Corresponding Author

*E-mail: cui@chem.wisc.edu.

Notes

The authors declare no competing financial interest.

■ ACKNOWLEDGMENTS

The research was supported in part by National Science Foundation Grant CHE-0957285. Computational resources from the National Center for Supercomputing Applications at the University of Illinois and the Center for High Throughput Computing (CHTC) at UW-Madison are greatly appreciated; computations are also supported in part by National Science Foundation through a major instrumentation grant (CHE-0840494). Discussions with Dr. Phillip Hünenberger and Mr. Gabriel Rocklin are acknowledged.

■ REFERENCES

(1) Honig, B.; Nicholls, A. Classical Electrostatics in Biology and Chemistry. *Science* **1995**, *268*, 1144−1149.

(2) Warshel, A.; Sharma, P. K.; Kato, M.; Parson, W. W. Modeling Electrostatic Effects in Proteins. *Biochim. Biophys. Acta* **2006**, *1764*, 1647−1676.

(3) Baker, N. A.; Sept, D.; Joseph, S.; Holst, M. J.; McCammon, J. A. Electrostatics of Nanosystems: Application to Microtubules and the Ribosome. *Proc. Natl. Acad. Sci. U.S.A.* **2001**, *98*, 10037−10041.

(4) Frenkel, D.; Smit, B. *Understanding Molecular Simulations: From Algorithms to Applications*; Academic Press, San Diego, CA, 1996.

(5) Darden, T.; York, D.; Pedersen, L. Particle Mesh Ewald: An Nlog(N) Method for Ewald Sums in Large Systems. *J. Chem. Phys.* **1993**, *98*, 10089−10092.

(6) Kuwajima, S.; Warshel, A. The Extended Ewald Method: A General Treatment of Long-Range Electrostatic Interactions in Microscopic Simulations. *J. Chem. Phys.* **1988**, *89*, 3751−3759.

(7) Bogusz, S.; Cheatham, T. E.; Brooks, B. R. Removal of Pressure and Free Energy Artifacts in Charged Periodic Systems via Net Charge Corrections to the Ewald Potential. *J. Chem. Phys.* **1998**, *108*, 7070−7084.

(8) Hünenberger, P. H.; McCammon, J. A. Ewald Artifacts in Computer Simulations of Ionic Solvation and Ion-Ion Interaction: A Continuum Electrostatics Study. *J. Chem. Phys.* **1999**, *110*, 1856−1872.

(9) Weber, W.; Hünenberger, P. H.; McCammon, J. A. Molecular Dynamics Simulations of a Polyalanine Octapeptide under Ewald Boundary Conditions: Influence of Artificial Periodicity on Peptide Conformation. *J. Phys. Chem. B* **2000**, *104*, 3668−3675.

(10) King, G.; Lee, F. S.; Warshel, A. Microscopic Simulations of Macroscopic Dielectric Constants of Solvated Proteins. *J. Chem. Phys.* **1991**, *95*, 4366−4377.
(11) Schutz, C. N.; Warshel, A. What Are the Dielectric "Constants" of Proteins and How To Validate Electrostatic Models? *Proteins: Struct., Funct., Genet.* **2001**, *44*, 400−417.
(12) Warshel, A.; Dryga, A. Simulating Electrostatic Energies in Proteins: Perspectives and Some Recent Studies of pK_as, Redox, and Other Crucial Functional Properties. *Proteins: Struct., Funct., Bioinf.* **2011**, *79*, 3469−3484.
(13) Im, W.; Bernèche, S.; Roux, B. Generalized Solvent Boundary Potential for Computer Simulations. *J. Chem. Phys.* **2001**, *114*, 2924−2937.
(14) Schaefer, P.; Riccardi, D.; Cui, Q. Reliable Treatment of Electrostatics in Combined QM/MM Simulation of Macromolecules. *J. Chem. Phys.* **2005**, *123*, 014905 1−14.
(15) Riccardi, D.; Schaefer, P.; Yang, Y.; Yu, H.; Ghosh, N.; Prat-Resina, X.; Konig, P.; Li, G.; Xu, D.; Guo, H.; Elstner, M.; Cui, Q. Development of Effective Quantum Mechanical/Molecular Mechanical (QM/MM) Methods for Complex Biological Processes (Feature Article). *J. Phys. Chem. B* **2006**, *110*, 6458−6469.
(16) Benighaus, T.; Thiel, W. Efficiency and Accuracy of the Generalized Solvent Boundary Potential for Hybrid QM/MM Simulations: Implementation for Semiempirical Hamiltonians. *J. Chem. Theory Comput.* **2008**, *4*, 1600−1609.
(17) Ge, X.; Roux, B. Absolute Binding Free Energy Calculations of Sparsomycin Analogs to the Bacterial Ribosome. *J. Phys. Chem. B* **2010**, *114*, 9525−9539.
(18) Yang, Y.; Yu, H.; Cui, Q. Extensive Conformational Changes are Required to Turn On ATP Hydrolysis in Myosin. *J. Mol. Biol.* **2008**, *381*, 1407−1420.
(19) Ghosh, N.; Prat-Resina, X.; Gunner, M. R.; Cui, Q. Towards a Reliable Molecular Model of Cytochrome c Oxdiase: Insights from Microscopic pK_a Calculations. *Biochemistry* **2009**, *48*, 2468−2485.
(20) Goyal, P.; Ghosh, N.; Phatak, P.; Clemens, M.; Gaus, M.; Elstner, M.; Cui, Q. Proton Storage Site in Bacteriorhodopsin: New Insights from QM/MM Simulations of Microscopic pK_a and Infrared Spectra. *J. Am. Chem. Soc.* **2011**, *133*, 14981−14997.
(21) Banavali, N. K.; Im, W.; Roux, B. Electrostatic Free Energy Calculations Using the Generalized Solvent Boundary Potential Method. *J. Chem. Phys.* **2002**, *117*, 7381−7388.
(22) Riccardi, D.; Schaefer, P.; Cui, Q. pK_a Calculations in Solution and Proteins with QM/MM Free Energy Perturbation Simulations: A Quantitative Test of QM/MM Protocols. *J. Phys. Chem. B* **2005**, *109*, 17715−17733.
(23) Riccardi, D.; Cui, Q. pK_a Analysis for the Zinc-Bound Water in Human Carbonic Anhydrase II: Benchmark for "Multi-Scale" QM/MM Simulations and Mechanistic Implications. *J. Phys. Chem. A* **2007**, *111*, 5703−5711.
(24) Simonson, T.; Perahia, D. Microscopic Dielectric Properties of Cytochrome c from Molecular Dynamics Simulations in Aqueous Solution. *J. Am. Chem. Soc.* **1995**, *117*, 7987−8000.
(25) Simonson, T.; Brooks, C. L., III. Charge Screening and the Dielectric Constant of Proteins: Insights from Molecular Dynamics. *J. Am. Chem. Soc.* **1996**, *118*, 8452−8458.
(26) Goh, G. B.; B. Garcia-Moreno, E.; Brooks, C. L., III. The High Dielectric Constant of Staphylococcal Nuclease Is Encoded in Its Structural Architecture. *J. Am. Chem. Soc.* **2011**, *133*, 20072−20075.
(27) Hummer, G.; Pratt, L. R.; Garca, A. E. Free Energy of Ionic Hydration. *J. Phys. Chem.* **1996**, *100*, 1206−1215.
(28) Figueirido, F.; Buono, G. S. D.; Levy, R. M. On Finite Size Effects in Computer Simulations Using the Ewald Potential. *J. Chem. Phys.* **1995**, *103*, 6133−6142.
(29) Hummer, G.; Pratt, L. R.; Garca, A. E. Electrostatic Potentials and Free Energies of Solvation of Polar and Charged Molecules. *J. Phys. Chem. B* **1997**, *101*, 3017−3020.
(30) Hummer, G.; Pratt, L. R.; Garca, A. E.; Garde, S.; Berne, B. J.; Rick, S. W. Reply to Comment on "Electrostatic Potentials and Free Energies of Solvation of Polar and Charged Molecules. *J. Phys. Chem. B* **1998**, *102*, 3841−3843.
(31) Åqvist, J.; Hansson, T. Analysis of Electrostatic Potential Truncation Schemes in Simulations of Polar Solvents. *J. Phys. Chem. B* **1998**, *102*, 3837−3840.
(32) Vorobjev, Y. N.; Hermans, J. A Critical Analysis of Methods of Calculation of a Potential in Simulated Polar Liquids: Strong Arguments in Favor of "Molecule-Based" Summation and of Vacuum Boundary Conditions in Ewald Summation. *J. Phys. Chem. B* **1999**, *103*, 10234−10242.
(33) Babu, C. S.; Yang, P.-K.; Lim, C. On the Charge and Molecule Based Summations of Solvent Electrostatic Potentials and the Validity of Electrostatic Linear Response in Water. *J. Biol. Phys.* **2002**, *2*, 95−113.
(34) Ashbaugh, H. S.; Wood, R. H. Effects of Long-Range Electrostatic Potential Truncation on the Free Energy of Ionic Hydration. *J. Chem. Phys.* **1997**, *106*, 8135−8139.
(35) Darden, T.; Pearlman, D.; Pedersen, L. G. Ionic Charging Free Energies: Spherical versus Periodic Boundary Conditions. *J. Chem. Phys.* **1998**, *109*, 10921−10935.
(36) Kastenholz, M. A.; Hünenberger, P. H. Computation of Methodology-Independent Ionic Solvation Free Energies from Molecular Simulations. I. The Electrostatic Potential in Molecular Liquids. *J. Chem. Phys.* **2006**, *124*, 124106 1−27.
(37) Reif, M. M.; Hünenberger, P. H.; Oostenbrink, C. New Interaction Parameters for Charged Amino Acid Side Chains in the GROMOS Force Field. *J. Chem. Theory Comp.* **2012**, *8*, 3705−3723.
(38) Yu, H.; Mazzanti, C. L.; Whitfield, T. W.; Koeppe, R. E.; Andersen, O. S.; Roux, B. A Combined Experimental and Theoretical Study of Ion Solvation in Liquid N-Methylacetamide. *J. Am. Chem. Soc.* **2010**, *132*, 10847−10856.
(39) Li, G.; Zhang, X.; Cui, Q. Free Energy Perturbation Calculations with Combined QM/MM Potentials Complications, Simplifications, and Applications to Redox Potential Calculations. *J. Phys. Chem. B* **2003**, *107*, 8643−8653.
(40) Olsson, M. H. M.; Hong, G.; Warshel, A. Frozen Density Functional Free Energy Simulations of Redox Proteins: Computational Studies of the Reduction Potential of Plastocyanin and Rusticyanin. *J. Am. Chem. Soc.* **2003**, *125*, 5025−5039.
(41) Cascella, M.; Magistrato, A.; Tavernelli, I.; Carloni, P.; Rothlisberger, U. Role of Protein Frame and Solvent for the Redox Properties of Azurin from Pseudomonas Aeruginosa. *Proc. Natl. Acad. Sci. U.S.A.* **2006**, *103*, 19641−19646.
(42) Simonson, T.; Carlsson, J.; Case, D. A. Proton Binding to Proteins: pK_a Calculations with Explicit and Implicit Solvent Models. *J. Am. Chem. Soc.* **2004**, *126*, 4167−4180.
(43) Simonson, T. Electrostatic Free Energy Calculations for Macromolecules: A Hybrid Molecular Dynamics/Continuum Electrostatics Approach. *J. Phys. Chem. B* **2000**, *104*, 6509−6513.
(44) Woo, H. J.; Roux, B. Calculation of Absolute Protein-Ligand Binding Free Energy from Computer Simulations. *Proc. Natl. Acad. Sci. U.S.A.* **2005**, *102*, 6825−6830.
(45) Levy, R. M.; Belhadj, M.; Kitchen, D. B. Gaussian Fluctuation Formula for Electrostatic Free Energy Changes. *J. Chem. Phys.* **1991**, *95*, 3627−3633.
(46) Simonson, T. Gaussian Fluctuations and Linear Response in an Electron Transfer Protein. *Proc. Natl. Acad. Sci. U.S.A.* **2002**, *99*, 6544−6549.
(47) Ghosh, N.; Cui, Q. pK_a of Residue 66 in *Staphylococal nuclease*. I. Insights from QM/MM Simulations with Conventional Sampling. *J. Phys. Chem. B* **2008**, *112*, 8387−8397.
(48) Warshel, A. *Computer Modeling of Chemical Reactions in Enzymes and Solution*; Wiley, New York, 1991.
(49) Kastenholz, M. A.; Hünenberger, P. H. Computation of Methodology-Independent Ionic Solvation Free Energies from Molecular Simulations. II. The Hydration Free Energy of the Sodium Cation. *J. Chem. Phys.* **2006**, *124*, 224501 1−20.
(50) Mackerell, A. D.; Bashford, D.; Bellott; Dunbrack, R. L.; Evanseck, J. D.; Field, M. J.; Fischer, S.; Gao, J.; Guo, H.; Ha, S.;

Joseph-McCarthy, D.; Kuchnir, L.; Kuczera, K.; Lau, F. T. K.; Mattos, C.; et al. All-Atom Empirical Potential for Molecular Modeling and Dynamics Studies of Proteins. *J. Phys. Chem. B* **1998**, *102*, 3586−3616.
(51) Jorgensen, W. L.; Chandrasekhar, J.; Madura, J. D.; Impey, R. W.; Klein, M. L. Comparison of Simple Potential Functions for Simulating Liquid Water. *J. Chem. Phys.* **1983**, *79*, 926−935.
(52) Berendsen, H. J. C.; Postma, J. P. M.; van Gunsteren, W. F.; Hermans, J. In *Intermolecular Forces*; Pullman, B., Ed.; Reidel: Dordrecht, 1981.
(53) Andersen, H. C. Molecular Dynamics Simulations at Constant Pressure and/or Temperature. *J. Chem. Phys.* **1980**, *72*, 2384−2393.
(54) Essmann, U.; Perera, L.; Berkowitz, M. L.; Darden, T.; Lee, H.; Pedersen, L. G. A Smooth Particle Mesh Ewald Method. *J. Chem. Phys.* **1995**, *103*, 8577−8593.
(55) Stote, R. H.; States, D. J.; Karplus, M. On the Treatment of Electrostatic Interactions in Biomolecular Simulations. *J. Chim. Phys.* **1991**, *88*, 2419−2433.
(56) Nosé, S. A Unified Formulation of the Constant Temperature Molecular Dynamics Methods. *J. Chem. Phys.* **1984**, *81*, 511−519.
(57) Hoover, W. G. Canonical Dynamics: Equilibrium Phase-Space Distributions. *Phys. Rev. A* **1985**, *31*, 1695−1697.
(58) Ryckaert, J.-P.; Ciccotti, G.; Berendsen, H. J. Numerical Integration of the Cartesian Equations of Motion of a System with Constraints: Molecular Dynamics of N-Alkanes. *J. Comput. Phys.* **1977**, *23*, 327−341.
(59) Štrajbl, M.; Hong, G.; Warshel, A. Ab Initio QM/MM Simulation with Proper Sampling: "First Principle" Calculations of the Free Energy of the Autodissociation of Water in Aqueous Solution. *J. Phys. Chem. B* **2002**, *106*, 13333−13343.
(60) Changela, A.; Chen, K.; Xue, Y.; Holschen, J.; Outten, C. E.; O'Halloran, T. V.; Mondragón, A. Molecular Basis of Metal-Ion Selectivity and Zeptomolar Sensitivity by CueR. *Science* **2003**, *301*, 1383−1387.
(61) Hobman, J. L. MerR Family Transcription Activators: Similar Designs, Different Specificities. *Mol. Microbiol.* **2007**, *63*, 1275−1278.
(62) Rao, L.; Cui, Q.; Xu, X. Electronic Properties and Desolvation Penalties of Metal Ions Plus Protein Electrostatics Dictate the Metal Binding Affinity and Selectivity in the Copper Efflux Regulator. *J. Am. Chem. Soc.* **2010**, *132*, 18092−18102.
(63) Brooks, B. R.; Brooks, C. L.; Mackerell, A. D.; Nilsson, L.; Petrella, R. J.; Roux, B.; Won, Y.; Archontis, G.; Bartels, C.; Boresch, S.; Caflisch, A.; Caves, L.; Cui, Q.; Dinner, A. R.; Feig, M.; et al. CHARMM: The Biomolecular Simulation Program. *J. Comput. Chem.* **2009**, *30*, 1545−1614.
(64) Im, W.; Beglov, D.; Roux, B. Continuum Solvation Model: Computation of Electrostatic Forces from Numerical Solutions to the Poisson-Boltzmann Equation. *Comput. Phys. Commun.* **1998**, *111*, 59−75.
(65) Nina, M.; Beglov, D.; Roux, B. Atomic Radii for Continuum Electrostatics Calculations Based on Molecular Dynamics Free Energy Simulations. *J. Phys. Chem. B* **1997**, *101*, 5239−5248.
(66) Beglov, D.; Roux, B. Finite Representation of an Infinite Bulk System: Solvent Boundary Potential for Computer Simulations. *J. Chem. Phys.* **1994**, *100*, 9050−9063.
(67) Lazaridis, T.; Karplus, M. Effective Energy Function for Proteins in Solution. *Proteins: Struct., Funct., Genet.* **1999**, *35*, 133−152.
(68) Goyal, P.; Cui, Q. Factors that Influence the pK_a of Glu286 in Cytochrome c Oxidase (*Rhodobacter sphaeroides*), manuscript in preparation, 2012.
(69) Woo, H.-J.; Dinner, A. R.; Roux, B. Grand Canonical Monte Carlo Simulations of Water in Protein Environments. *J. Chem. Phys.* **2004**, *121*, 6392−6400.
(70) Chakrabarty, S.; Warshel, A. Capturing the Energetics of Water Insertion in Biological Systems: The Water Flooding Approach. *Proteins: Struct., Funct., Bioinf.* **2013**, *81*, 93−106.
(71) Song, X. An Inhomogeneous Model of Protein Dielectric Properties: Intrinsic Polarizabilities of Amino Acids. *J. Chem. Phys.* **2002**, *116*, 9359−9363.
(72) Benighaus, T.; Thiel, W. A General Boundary Potential for Hybrid QM/MM Simulations of Solvated Biomolecular Systems. *J. Chem. Theory Comput.* **2009**, *5*, 3114−3128.
(73) Zienau, J.; Cui, Q. Implementation of the Solvent Macromolecule Boundary Potential and Application to Model and Realistic Enzyme Systems. *J. Phys. Chem. B* **2012**, *116*, 12522−12534.